

**SSA and  
heterogeneous  
chemistry in polluted  
coastal areas**

E. Athanasopoulou et al.

# The role of sea-salt emissions and heterogeneous chemistry in the air quality of polluted coastal areas

**E. Athanasopoulou<sup>1</sup>, M. Tombrou<sup>1</sup>, S. N. Pandis<sup>2</sup>, and A. G. Russell<sup>3</sup>**

<sup>1</sup>National and Kapodistrian University of Athens, Faculty of Physics, Dep. of Environmental Physics and Meteorology, Athens, Greece

<sup>2</sup>Department of Chemical Engineering, University of Patras, 26500 Patra, Greece

<sup>3</sup>School of Civil and Environmental Engineering, Georgia Institute of Technology, 311 Ferst Drive NW, Atlanta, GA 30332-0512, USA

Received: 3 January 2008 – Accepted: 22 January 2008 – Published: 25 February 2008

Correspondence to: E. Athanasopoulou (eathana@phys.uoa.gr)

Published by Copernicus Publications on behalf of the European Geosciences Union.

Title Page

Abstract

Introduction

Conclusions

References

Tables

Figures

⏪

⏩

◀

▶

Back

Close

Full Screen / Esc

Printer-friendly Version

Interactive Discussion

## Abstract

Open-ocean and surf-zone sea-salt aerosol (SSA) emissions algorithms are incorporated in the CAMx aerosol model and applied over an area with an extended Archipelago (Greece), with a fine grid nested over the highly populated Attica peninsula. The maximum indirect impact of SSA on PM<sub>10</sub> mass (35%) is located over a marine area with moderate SSA production and elevated shipping emissions (central Aegean Sea) where SSA interacts with anthropogenic nitric acid forming sodium nitrate. SSA increases PM<sub>10</sub> levels in the Athens city center up to 27% during stable onshore winds. Under such conditions both open-ocean and surf-zone mechanisms contribute to aerosol production over Attica. A hybrid scheme for gas-to-particle mass transfer is necessary for accurately simulating semi-volatile aerosol components when coarse SSA is included. Dynamically simulating mass transfer to the coarse particles leads to a quadrupling of predicted PM<sub>10</sub> nitrate in the Athens city center and up to two orders of magnitude in its coarse mass in comparison to using a bulk equilibrium approach.

## 1 Introduction

Sea salt is one of the major atmospheric aerosol components on a global scale (Lewis and Schwartz, 2004) and can significantly impact particulate matter concentrations in coastal locations. Sea-salt aerosol (SSA) is mainly produced by bursting bubbles during whitecap formation in the open-ocean (Monahan et al., 1986). A more localized mechanism of SSA production involves waves breaking in the surf zone. This mechanism may affect areas even at a distance of 25 km from the coastline and can dominate the coastal SSA levels (Monahan, 1995; De Leeuw et al., 2000; Woodcock et al., 1963).

The diameter of SSA ranges from less than 0.2  $\mu\text{m}$  to greater than 2000  $\mu\text{m}$ . The ambient SSA mass distribution is dominated by particles in the 1–10  $\mu\text{m}$  diameter range.

ACPD

8, 3807–3841, 2008

## SSA and heterogeneous chemistry in polluted coastal areas

E. Athanasopoulou et al.

Title Page

Abstract

Introduction

Conclusions

References

Tables

Figures

⏪

⏩

◀

▶

Back

Close

Full Screen / Esc

Printer-friendly Version

Interactive Discussion

---

**SSA and  
heterogeneous  
chemistry in polluted  
coastal areas**E. Athanasopoulou et al.

---

[Title Page](#)[Abstract](#)[Introduction](#)[Conclusions](#)[References](#)[Tables](#)[Figures](#)[⏪](#)[⏩](#)[◀](#)[▶](#)[Back](#)[Close](#)[Full Screen / Esc](#)[Printer-friendly Version](#)[Interactive Discussion](#)

In a typical urban atmosphere, measured mass size distributions of sodium and chloride concentrations show a dominant peak around  $4\ \mu\text{m}$  (Wall et al., 1988). Particles smaller than  $1\ \mu\text{m}$  can make substantial contributions to cloud condensation nuclei concentrations (Pierce and Adams, 2006), while particles larger than  $50\ \mu\text{m}$  have a very short atmospheric life and play a negligible role in atmospheric chemistry (Lewis and Schwartz, 2004).

SSA participates in atmospheric chemistry by interacting with atmospheric pollutants. For example, sodium chloride in polluted areas (e.g. cities or areas with ship-routes) reacts with sulfuric and nitric acid producing sodium sulfate and nitrate together with hydrochloric acid gas. The timescale of these reactions with coarse SSA can be several hours (Meng and Seinfeld, 1996) and leads to a chloride “deficit” in the SSA (Seinfeld and Pandis, 1998). As sea-salt particles are transported inland during periods with onshore winds, they compete with the fine aerosol particles for sulfuric and nitric acid changing both the concentration and size distribution of the corresponding sulfate, nitrate and chloride salts.

The first atmospheric aerosol thermodynamics modules (EQUIL, KEQUIL, MARS, MARS-A) neglected the role of sea-salt, and focused on the sulfate-nitrate-ammonium-water system (Bassett and Seinfeld, 1983; 1984; Saxena et al., 1986; Binkowski and Shankar, 1995). This can lead to errors in the simulated chemical composition of aerosol and the related gas-phase species, especially for coastal and marine-affected areas (Bessagnet et al., 2004; Hodzic et al., 2006). The second generation of such modules (e.g. SEQUILIB, SCAPE, EQUISOLV, ISORROPIA and ISORROPIAII) describes the interactions among sodium and chloride and the rest of the major inorganic aerosol species (Nenes et al., 1998; Zhang et al., 2000; Fountoukis and Nenes, 2007). Nevertheless, even models incorporating such modules can underestimate  $\text{PM}_{10}$  aerosol mass in coastal areas when they do not include SSA emissions (Mebust et al., 2003). Errors can also occur when models assume instantaneous mass transfer between the gas and condensed phases in areas with high sea-salt concentrations (Lurmann et al., 1997). Capaldo et al. (2000) argued that in these cases the total ni-

trate concentration is underestimated and the nitrate distribution is biased towards the fine aerosol.

Several authors have proposed parameterizations for sea-salt emissions fluxes (Ling et al., 1980; Gathman, 1982; Blanchard, 1963; Fairall et al., 1983; Monahan et al., 1986; Bortkovskii, 1987; Woolf et al., 1988; Andreas, 1992; Iida et al., 1992; Wu, 1992; Smith et al., 1993; O'Dowd et al., 1997; Andreas, 1998; Smith and Harrison, 1998; De Leeuw et al., 2000; Hoppel et al., 2002; Martensson et al., 2003; Gong, 2003; Clarke et al., 2006). These expressions typically calculate the number flux density of SSA as a function of the wind speed at 10 m ( $U_{10}$ ) above sea level and at a specific ambient relative humidity (usually  $RH=80\%$ ). Martensson et al. (2003) is an exception and includes a temperature dependence and O'Dowd et al. (1997) specify the concentration rather than the emissions flux. Parameterization applicability depends on SSA size range and wind speed. Almost all source functions predict open-ocean produced aerosol, except DEL00 (De Leeuw et al., 2000), which is a surf-zone parameterization. CL06 (Clarke et al., 2006) is the only parameterization that covers sub-micron particles; Monahan et al. (1986) is applicable to a relatively narrow size range but was extended to smaller sizes by G-M03 (Gong, 2003).

A number of attempts have been made to incorporate SSA source functions in atmospheric models. Most applications are on a global scale (Alexander et al., 2005; Gong et al., 1997; Witek et al., 2007; Pierce and Adams, 2006; Vignati et al., 2001; Gong, 2003), while a few studies refer to regional, though low resolution applications (Spyridaki et al., 2006; Foltescu et al., 2004). The most commonly used source function is that of Monahan et al. (1986), while no surf-zone modeling applications exist.

Pierce and Adams (2006) showed an increase in predicted CCN concentrations due to the incorporation of sea-salt emissions, though these values are quite sensitive to the mean wind speeds and distributions. Witek et al. (2007) reported good correlation between SSA simulation results and data from shipboard experiments, although their predictions were higher. This over-prediction increased at high wind speeds. Higher sodium predictions at marine-affected ground stations in Northern Europe were also

---

## SSA and heterogeneous chemistry in polluted coastal areas

E. Athanasopoulou et al.

---

Title Page

Abstract

Introduction

Conclusions

References

Tables

Figures

⏪

⏩

◀

▶

Back

Close

Full Screen / Esc

Printer-friendly Version

Interactive Discussion

---

**SSA and  
heterogeneous  
chemistry in polluted  
coastal areas**

---

E. Athanasopoulou et al.

---

[Title Page](#)[Abstract](#)[Introduction](#)[Conclusions](#)[References](#)[Tables](#)[Figures](#)[⏪](#)[⏩](#)[◀](#)[▶](#)[Back](#)[Close](#)[Full Screen / Esc](#)[Printer-friendly Version](#)[Interactive Discussion](#)

reported by Foltescu et al. (2004), who stressed the model's difficulty in capturing deposition in complex terrain, the coarse particle sampling difficulties, as well as mass differences caused by area-to-point comparisons. On the other hand, Spyridaki et al. (2006) found under-predictions of marine aerosol species over the southeastern part of Greece, probably due to underestimation of sea-salt boundary concentrations. Shankar et al. (2006) have concluded that SSA contributes substantially to sulfate and nitrate concentrations. This effect was underestimated by their model due to the underestimation of the fine SSA production by the Gong (2003) source function and to the exclusion of surf-zone emissions from the applied parameterization. The latter is further stressed by the study of Vignati et al. (2001), which concludes that surf-zone aerosol provides additional surface for heterogeneous reactions and greatly impacts marine-affected areas. Another issue is that grid cells of the regional models cause an artificial smoothing of the coastline and of the surf-zone width, leading to inaccuracies in the calculation of surf-zone emissions.

This paper describes the incorporation of a comprehensive SSA parameterization in the CAMx aerosol model (Environ, 2004). The main goal is to examine the role of SSA in the atmospheric chemistry over an area with an extended Archipelago. The selected area for model application is Greece, situated in the southeastern Mediterranean. The grid system used combines a high-resolution nested domain over Attica peninsula with a parent domain over Greece and surrounding areas and the applied SSA emission algorithms describe both open-ocean and surf-zone particle production. The system is then used to investigate SSA contributions to aerosol mass together with chemical interactions between sea salt and atmospheric pollutants. Additionally, the effectiveness of the open-ocean versus surf-zone production mechanisms is investigated. Finally, it is examined whether is crucial to dynamically model the gas-to-particle conversion of condensable material when it contains semi-volatile ions (chloride, nitrate).

## 2 Air quality model

CAMx is a 3-D, Eulerian chemical transport model. The version of the model used in this study (4.11 s) uses the CB-IV gas-phase chemical mechanism (Gery et al., 1989), the RADM algorithm for cloud chemistry (Chang et al., 1987), the SOAP scheme for the organic species partitioning (Strader et al., 1998) and ISORROPIA for the thermodynamic equilibrium of inorganic aerosol (Nenes et al., 1998). The system treated by ISORROPIA includes sodium ( $\text{Na}^+$ ), ammonium ( $\text{NH}_4^+$ ), chloride ( $\text{Cl}^-$ ), sulfate ( $\text{SO}_4^{2-}$ ), nitrate ( $\text{NO}_3^-$ ) and water ( $\text{H}_2\text{O}$ ), which are partitioned between gas, liquid and solid phases. Sulfate and sodium completely reside in the aerosol phase, while other aerosol species are found in both phases, based largely on the value of sulfate and sodium molar ratio ( $\text{Na}^+ + \text{NH}_4^+ / \text{SO}_4^{2-}$  and  $\text{Na}^+ / \text{SO}_4^{2-}$ , respectively).

Mass transfer between gas and aerosol phases is calculated using the hybrid approach (Capaldo et al., 2000), which assumes instantaneous equilibrium between gases and fine aerosols (equilibrium approach) and solves the mass transfer rate equations for the coarse mass (dynamic approach). Fine particles achieve equilibrium with the gas phase within a few minutes while tens of minutes or even hours are necessary for the equilibration of coarse particles. The threshold diameter between the two approaches was set at  $2.5 \mu\text{m}$  in this study, in order to achieve both speed and accuracy during simulations (Capaldo et al., 2000; Koo et al., 2003).

CAMx employs a sectional approach for the aerosol mass distribution between  $0.04$  and  $40 \mu\text{m}$  (particle diameter). Ten discrete and internally mixed size sections (bins), each consisting of thirteen chemical aerosol components (primary: organic and elemental carbon, chloride, sodium, sulfate ions and crustal material; secondary: four organics, water, ammonium, nitrate and sulfate ions) lead to 130 aerosol “species” treated by the model.

Title Page

Abstract

Introduction

Conclusions

References

Tables

Figures

⏪

⏩

◀

▶

Back

Close

Full Screen / Esc

Printer-friendly Version

Interactive Discussion

### 3 Method

#### 3.1 Modeling domain

The CAMx simulation area covers the greater Greece area (parent domain) using a spatial resolution of 6 km, while a finer resolution of 2 km is used in the nested domain centered on the Attica peninsula (Fig. 1). The areas of the parent and the nested domain are 777 924 km<sup>2</sup> (147×147 cells) and 21600 km<sup>2</sup> (75×72 cells), respectively. In the vertical, the physical layer height structure consists of 14 levels up to 5.1 km, with the top of the first layer approximately at 72 m.

Greece has an extended coastline and a large number of islands, making it an ideal case for the study of sea salt effects produced from open-ocean and surf-zone production mechanisms. Greece can be divided into four types of environments with respect to SSA and anthropogenic emissions: 1) low emission offshore areas with elevated SSA emissions, 2) offshore areas with SSA and sea-transport (shipping) emissions, 3) inland areas near the coastline, with emissions due to urban and industrial activities and 4) non-coastal inland areas less affected by SSA. The most representative area for the third case is in the Attica peninsula, where Athens is situated and is surrounded by an airport, three harbors and many industrial sources.

#### 3.2 Meteorology

Meteorological fields used in CAMx are produced by the fifth generation Penn State/NCAR Mesoscale Model, MM5 (Anthes and Warner, 1978). The applied version involves improved descriptions of the urban characteristics (Dandou et al., 2005). MM5 meteorological output is used to generate the CAMx input fields using the pre-processor “mm5camx-v4.2” (<http://www.camx.com/down/support.php>). The vertical diffusivity ( $K_v$ ) profiles can be calculated by different methods. Sensitivity runs revealed that the O'Brien (1970) parameterization produced more realistic first layer  $K_v$  values compared to that of Byun et al. (1999) in this application.

Title Page

Abstract

Introduction

Conclusions

References

Tables

Figures

⏪

⏩

◀

▶

Back

Close

Full Screen / Esc

Printer-friendly Version

Interactive Discussion

---

**SSA and  
heterogeneous  
chemistry in polluted  
coastal areas**E. Athanasopoulou et al.

---

Title Page

Abstract

Introduction

Conclusions

References

Tables

Figures

⏪

⏩

◀

▶

Back

Close

Full Screen / Esc

Printer-friendly Version

Interactive Discussion

The modeling system is applied for a summer open anti-cyclonic (OA) event. OA synoptic conditions frequently occur over Greece ( $38\% \text{ yr}^{-1}$ ), are usually clear and sunny and are characterized by relatively weak wind flows that favor development of sea-breeze circulation over the Athens basin during summer (Kassomenos et al., 1998; Melas et al., 1998; Ziomias et al., 1995). During the day examined in detail, West-North West (WNW) wind speed maxima (about  $11 \text{ m s}^{-1}$ ) are predicted around the island of Crete, while lower wind speed values (up to  $4 \text{ m s}^{-1}$ ) are predicted north of Crete (Cyclades islands area). Winds from the south sector are constant over the central and northern Aegean Sea. The Attica peninsula is affected by the WNW flow (about  $7 \text{ m s}^{-1}$ ) during the early morning and night hours and by a SSW flow during the rest of the day. SSW flow is intensified by the air-mass entrainment from the Cyclades area (southern boundary) and is fully developed during the afternoon (about  $6 \text{ m s}^{-1}$ ).

### 3.3 Initial and boundary conditions

Initial and boundary conditions for the day examined (24 June 1998) are assumed to be spatially and temporally invariant for the parent domain. The concentrations for the main gaseous pollutants are typical values for the area during the warm period, i.e. 50 ppb for CO, 1 ppb for  $\text{NO}_x$ , 3 ppb for  $\text{SO}_2$  and 40 ppb  $\text{O}_3$ . For the rest of the gaseous species, lower bound concentrations are automatically set by the model ( $10^{-6}$  ppb). The simulated synoptic condition (OA) does not have southern winds that favor African dust transport in the Mediterranean atmosphere, and this was confirmed by satellite imagery for the specific days ([http://toms.gsfc.nasa.gov/eptoms/ep\\_v8.html](http://toms.gsfc.nasa.gov/eptoms/ep_v8.html)), thus the default aerosol boundary concentrations are used for this study ( $10^{-9} \mu\text{g m}^{-3}$ ). Tests showed that sea salt boundary conditions have a significant aerosol impact to only about 20 km into the domain, thus default values are again acceptable.

In order to avoid the transient effects associated with initial conditions, we use a 3-day “spin-up” modeling period. Sensitivity tests of CAMx have indicated that this 3-day start-up period is sufficient to minimize the role of initial conditions on aerosol

concentrations for the parent domain.

#### 4 Emissions – Implementation of SSA in the model

Hourly emissions of NO<sub>x</sub>, SO<sub>2</sub>, NMVOC, CO, NH<sub>3</sub>, isoprene, terpenes and bulk PM<sub>10</sub> from Greek industries, road transport, maritime activities, railways, air traffic, agricultural activities and forests were provided by the Greek Ministry of the Environment for a typical summer and a winter weekday of 2002. The NMVOC emissions speciation profiles used here are described by Bossioli et al. (2002). The spatial distribution of anthropogenic emissions shows the importance of both on-shore and shipping emissions (Fig. 2). Seasonal NH<sub>3</sub> emissions from agricultural activities were provided by Sotiropoulou et al. (2003) for the Attica area. This information was then combined with the land type database to estimate NH<sub>3</sub> emission rates from forest, agricultural and range land types which were then applied to the rest area of Greece. Hourly NH<sub>3</sub> emission rates follow the daily temperature variation over Attica.

PM<sub>10</sub> dust emission factors for road abrasion and tire/brake wear per vehicle were based on IIASA (<http://www.iiasa.ac.at/~rains/PM>). This information was then combined with the spatial-temporal distribution of vehicles and the NO<sub>x</sub> traffic emissions distribution. Bulk PM<sub>10</sub> mass rates, by source, were split into 5 chemical species and distributed by size, according to literature review (CARB database: <http://www.arb.ca.gov/ei/speciate/dnldopt.htm>; SPECIATE (version 3.2) software: <http://www.epa.gov/ttn/chief/software/speciate/speciate32.html>; TNO/CEPMEIP database: [http://www.air.sk/tno/cepmeip/em\\_factors.php](http://www.air.sk/tno/cepmeip/em_factors.php); EMPA, 2000) (Fig. 3). Transportation sources emit mostly fine aerosol mass (PM<sub>2.5</sub>) comprised mainly of elemental carbon and organic PM, while re-suspended mass (from soil or roads) is mostly coarse inorganic and entails with a small amount of secondary nitrates. Point aerosol emissions distribute more evenly to the size bins and are mainly inorganic (sulfates and crustal material).

### SSA and heterogeneous chemistry in polluted coastal areas

E. Athanasopoulou et al.

Title Page

Abstract

Introduction

Conclusions

References

Tables

Figures

⏪

⏩

◀

▶

Back

Close

Full Screen / Esc

Printer-friendly Version

Interactive Discussion

## 4.1 Implementation of SSA in the model

The SSA emission parameterizations implemented in this study combines the CL06 source function for submicron particles and G-M03 for the larger particles (Table 1). Both equations are applied in the open-ocean cells of both domains. DEL00 is used for the parameterization of the surf-produced SSA and is applied at the coastal cells (land cells adjacent to cells covered totally by sea). The original source functions were adjusted to ambient RH (45–99%, as predicted by MM5) and salinity ( $S=38.5$ ) for the Mediterranean Sea conditions (Lewis and Schwartz, 2004) by using the correction factors ( $C_0$ ,  $C_{80}$ ) proposed by Zhang et al. (2005ab) and Lewis and Schwartz (2006). Additionally, the conversion factor of number to mass fluxes of aerosol (NM) depends on particle density ( $\rho$ ) and solute weight fraction ( $x$ ), as defined by Zhang et al. (2005a).

SSA emissions were split into the ten size bins of the model application (up to  $40\ \mu\text{m}$  in diameter), each having the seawater mass chemical composition (55%  $\text{Cl}^-$ , 8% sea-salt sulfate ( $\text{ss-SO}_4^-$ ), 6%  $\text{Mg}^+$ ,  $\text{Ca}^+$ ,  $\text{K}^-$ , and  $\text{Br}^-$  and  $\text{Cl}^-/\text{Na}^+=1.8$ ), which is acceptable for short times after SSA emission (Seinfeld and Pandis, 1998; Lewis and Schwartz, 2004). The surf-zone is assumed to cover 0.25% of the area of each coastal cell ( $0.01\ \text{km}^2$  for the nested domain), as no other information is available. This rather conservative value could correspond to a surface of 200 m coastline and 50 m surf-zone width for the nested domain. The value of 50 m is considered a mean surf-zone width (De Leeuw et al., 2000; Lewis and Schwartz, 2004).

The SSA emissions algorithm provides the spatial distribution of the hourly rates over the parent and nested domains (Fig. 4). The areas of highest SSA emissions, due to the wind speed distribution, are in the Southern Aegean (around Crete), while small values are predicted in the central and northern Aegean Sea. SSA  $\text{PM}_{10}$  emissions are similar in magnitude to the rest of the aerosol emission rates (not shown) over the nested domain and are larger over the parent domain. Open-ocean emissions are more important over offshore areas of the parent domain. In the central Aegean Sea, the open-ocean aerosol production is of equivalent importance to the surf-zone

Title Page

Abstract

Introduction

Conclusions

References

Tables

Figures

◀

▶

◀

▶

Back

Close

Full Screen / Esc

Printer-friendly Version

Interactive Discussion

mechanism due to the complex and long coastline. Over the nested domain, the surf-zone mechanism produces most of the SSA mass, although the surface from which it originates is small.

At a 10 m-wind speed ( $U_{10}$ ) of  $13 \text{ m s}^{-1}$ , SSA with diameters greater than  $0.6 \mu\text{m}$  and up to  $40 \mu\text{m}$  comprises 95% of the particle mass, but only 2% of the particle number (Fig. 5). For the same wind speed and surface area, surf-zone SSA emissions are about two orders of magnitude greater than SSA coming from open-ocean. The size range of the calculated surf-produced aerosol is narrow (De Leeuw et al., 2000; Lewis and Schwartz, 2004).

RH affects the size range of SSA emissions for both production mechanisms (Fig. 5). In particular, the doubling of RH almost doubles SSA sizes, thus under highly humid conditions (RH greater than 90%) little particle mass has diameters less than  $1 \mu\text{m}$  and it is uniquely produced from the open-ocean. SSA with diameters below  $10 \mu\text{m}$  is produced by both mechanisms (and not just from the open-ocean) only when RH is below 70%. SSA particles larger than  $40 \mu\text{m}$  are of minimal importance because production typically does not exceed  $30 \mu\text{m}$  (even when RH is 95%), but even when it does (spume droplets production) it comes from open-ocean mechanisms and particles deposit rapidly.

Over the surf-zone, minimum  $U_{10}$  values produce about  $1 \times 10^{-4} \text{ g m}^{-2} \text{ s}^{-1}$  SSA, which exponentially increases up to  $1.7 \times 10^{-3} \text{ g m}^{-2} \text{ s}^{-1}$  when  $U_{10}$  reaches the maximum calculated coastal value of  $12.3 \text{ m s}^{-1}$  (Fig. 6). SSA mass fluxes at two coastal sites in California were measured between  $3 \times 10^{-4}$  and  $1 \times 10^{-3} \text{ g m}^{-2} \text{ s}^{-1}$  for wind speeds lower than  $9 \text{ m s}^{-1}$  (De Leeuw et al., 2000). This similarity is expected, as DEL00 is based on these experimental data. The variation of wind speed affects the open-ocean SSA production more than the surf zone. In particular, although insignificant amounts of SSA mass are emitted during calm conditions, the maximum calculated wind speed ( $13 \text{ m s}^{-1}$ , for the selected event) results in  $2.5 \times 10^{-6} \text{ g m}^{-2} \text{ s}^{-1}$ . A prior approximation for open-ocean SSA emissions for the SE Greece (Alexandropoulou and Lazaridis, 2003) gave similar results.

## SSA and heterogeneous chemistry in polluted coastal areas

E. Athanasopoulou et al.

Title Page

Abstract

Introduction

Conclusions

References

Tables

Figures

⏪

⏩

◀

▶

Back

Close

Full Screen / Esc

Printer-friendly Version

Interactive Discussion

## 5 Model results

The hybrid method is used for calculating mass transfer between the gas and condensed phases in the base-case simulation and is compared to available data from the literature and to the bulk-equilibrium approach. In order to isolate and examine the impact of SSA production on  $PM_{10}$  concentrations and composition, additional simulations are performed with zero SSA emissions. Additional simulations address the relative importance of open-ocean and surf-zone SSA production. To examine the boundary entrainment of SSA into the nested domain from the parent domain, a test case calculated the SSA concentrations, assuming no SSA emissions in the parent domain.

### 5.1 Comparison of Simulated and Observed Concentrations

While particulate matter compositional data is not available for the period simulated, comparing these results with observations for similar conditions shows good agreement for  $Na^+$ ,  $Cl^-$  and sulfate (Fig. 7a, b, c, f). For example, the simulated average  $PM_{10}$   $Na^+$  concentrations in central Athens and Crete (Finokalia) are  $0.8 \mu g m^{-3}$  and  $2.3 \mu g m^{-3}$ , respectively, values consistent with measured values in previous field campaigns (Table 2). Chloride and sulfate predictions and observations are also similar. These results suggest that the SSA emissions algorithms provide reasonable mass fluxes.

Nitrate and ammonium mass is underestimated (Fig. 7d, e). Simulated  $PM_{10}$  nitrate average values are less than  $1 \mu g m^{-3}$ , on average, in Athens, Finokalia and Thessaloniki, while available measurements in similar summer periods suggest greater values (Table 2). Given the significant  $HNO_3$  simulated (around  $5 \mu g m^{-3}$ , Fig. 7g; observations are not available), this suggests that gas-to-particle conversion is underestimated. Ammonium predictions are around  $1 \mu g m^{-3}$ , for the whole  $PM_{10}$  mass, while observations exceed  $2 \mu g m^{-3}$  for  $PM_{2.5}$ , alone. Uncertainties in  $NH_3$  emissions are believed to play an important role in the above discrepancies. Ammonia predictions (Fig. 7h) are

Title Page

Abstract

Introduction

Conclusions

References

Tables

Figures

◀

▶

◀

▶

Back

Close

Full Screen / Esc

Printer-friendly Version

Interactive Discussion



extremely low (typically around  $10^{-2} \mu\text{g m}^{-3}$ ), and this leads to negligible production of fine  $\text{NH}_4\text{NO}_3$ , as also found by Athanasopoulou et al. (2005). The high marine-related  $\text{NO}_3^-$  and an absence of submicrometer  $\text{NO}_3^-$  is seen in other studies over marine areas (Bardouki et al., 2003; Eleftheriadis et al., 1998a; 1999). Lack of local dust emissions and their interaction with nitric acid, can also lead to nitrate underestimation (Hien et al., 2005; Hodzic et al., 2006). Such results suggest that the SSA,  $\text{SO}_2$  and  $\text{NO}_x$  emissions, and the oxidation of  $\text{SO}_2$  and  $\text{NO}_x$ , are captured, but that the ammonia emissions are low.

## 5.2 Impact of SSA on aerosol concentrations and composition

The difference in  $\text{PM}_{10}$  results between the base-case simulation and the simulation without SSA emissions (expressed as a percentage of the base-case concentrations) provides both the direct (addition of sea-salt) and indirect (heterogeneous reactions with sulfuric and nitric acid) effects of SSA in the  $\text{PM}_{10}$  concentrations in the area. Marine-affected  $\text{PM}_{10}$  is highest in the south (around  $30 \mu\text{g m}^{-3}$ ), with the rest of the mass mainly in the form of sulfate (Fig. 7f, i). At coastal sites, the fraction of  $\text{PM}_{10}$  from SSA and its reaction products ranges from 20 to 60% and is calculated 37% ( $6.5 \mu\text{g m}^{-3}$ ) at the coastal site of Piraeus. Experimental data ( $\text{Na}^+$ ,  $\text{Cl}^-$  and  $\text{ss-SO}_4^-$  species) from a coastal site in Spain (Salvador et al., 2007) indicate a similar  $\text{PM}_{10}$  contribution. SSA production also affects the aerosol inland, especially under onshore winds. For example, marine-related aerosol comprises a fourth of  $\text{PM}_{10}$  mass in the Athens basin ( $2.5 \mu\text{g m}^{-3}$ ), 9 km inland and diminishes to 13% ( $1 \mu\text{g m}^{-3}$ ) at Thrakomakedones, 27 km inland. SSA contributions to  $\text{PM}_{2.5}$  mass are much lower and in the Athens basin are around 10%.

Sodium is well suited to characterize SSA as it completely resides in the condensed phase and is dominated by sea emissions. Offshore areas away from the coastline are primarily affected by the open-ocean aerosol production mechanism. Over coastal areas, surf-zone mechanism is also important (Cyclades islands) or more important

## SSA and heterogeneous chemistry in polluted coastal areas

E. Athanasopoulou et al.

Title Page

Abstract

Introduction

Conclusions

References

Tables

Figures

⏪

⏩

◀

▶

Back

Close

Full Screen / Esc

Printer-friendly Version

Interactive Discussion

(Attica coastal zone) than open-ocean aerosol production. Over inland areas affected by stable onshore winds (e.g. Attica) open-ocean and surf-zone mechanisms contribute almost equally on aerosol production (Fig. 7a, b).

Low emission offshore areas away from the coastline find the chemical composition of the portion of aerosol mass linked to SSA, mainly (95%) as primary sea-salt ions ( $\text{Na}^+$ ,  $\text{Cl}^-$ ,  $\text{ss-SO}_4^-$ ,  $\text{Mg}^{2+}$ ,  $\text{Ca}^{2+}$ ,  $\text{K}^+$ ,  $\text{Br}^-$  etc), as chlorine remains mostly in the condensed phase (southern Aegean site in Fig. 8). Secondary aerosol production from reactions between SSA and nitric and sulfuric acid is minimal in these areas. Alternatively, in the Cyclades area (e.g., Delos island in Fig. 8), shipping routes are quite dense (Fig. 2) resulting in significant production of  $\text{HNO}_3$  which reacts with SSA forming  $\text{NaNO}_3$ . Here, primary sea-salt ions constitute 64% of marine-related  $\text{PM}_{10}$ , and aerosol  $\text{NO}_3^-$  another 32%. Aerosol  $\text{Cl}^-$  is displaced and the resulting  $\text{HCl}$  is lost by dry deposition. In the Attica peninsula, marine-related secondary species ( $\text{NO}_3^-$ ,  $\text{SO}_4^-$  and  $\text{NH}_4^+$ ) take lower concentration values as we move further north and inland, but are of greater importance, reaching 32% of the marine-affected aerosol at Thrakomakedones (N. suburb).

Simulated peak nitrate concentrations ( $4.5 \mu\text{g m}^{-3}$ ) occur over the marine area north of Crete (Fig. 7d) due to high local  $\text{NO}_x$  emissions from shipping, reduced deposition and the availability of  $\text{Na}^+$ , especially during early morning hours. As the day passes, peak values decrease by 2 to  $3 \mu\text{g m}^{-3}$ , but expand spatially. Winds transport nitrate into Attica from the southern sector, leading to a peak over the Saronic Gulf during the evening hours. Secondary peaks, near Eleusis and at the Evoikos Gulf, coincide with high  $\text{Na}^+$  ratios and local industrial sources emitting  $\text{NO}_x$  (Fig. 2b). The effect of SSA on  $\text{NO}_3^-$  over the Athens basin is also apparent (embedded rectangle in Fig. 7d) and follows the spatial distribution of  $\text{NO}_x$  emissions (Fig. 2) and of the wind-driven SSA mass. Use of the finer grid in this region allowed capturing the importance of surf-zone SSA production and relatively rapid chemical dynamics and gas-to-particle conversion near the coast.

Inclusion of SSA can also dramatically impact the formation of ammonium nitrate

## SSA and heterogeneous chemistry in polluted coastal areas

E. Athanasopoulou et al.

Title Page

Abstract

Introduction

Conclusions

References

Tables

Figures

⏪

⏩

◀

▶

Back

Close

Full Screen / Esc

Printer-friendly Version

Interactive Discussion

when liquid aerosol is present. In Thessaloniki, in the morning hours around rush hour, significantly more ammonium nitrate is simulated to be formed when SSA is included because the presence of additional salts (particularly sodium and the sulfate and nitrate that has reacted with chloride), in the small particles reduces the equilibrium constant between ammonia and nitric acid and increases the amounts found in the liquid drops.

### 5.3 Sensitivity to mass transfer between phases

Bulk  $PM_{10}$  predictions are affected by the treatment of mass transfer between the gas and condensed phases, but can have a dramatic effect on specific constituents. The difference in the inorganic  $PM_{10}$  results of the base-case simulation and the simulation with the bulk-equilibrium approach (expressed as a percentage of the base-case concentrations) reaches 10% over the central Aegean area (not shown), coinciding with elevated aerosol nitrate concentrations (Fig, 9). The chloride replacement by nitric acid is more extensive using the dynamic approach, while the bulk-equilibrium approach finds most chloride being displaced by  $H_2SO_4$ , leading to little production of sulfates, the rest NaCl remains inert, leading to little nitrate. Concentrations of HCl(g) are low in the bulk-equilibrium approach. This leads to large differences (up to 90%) in inorganic  $PM_{10}$  nitrate concentrations between the base-case simulation and that with the bulk-equilibrium approach over most of the marine-affected domain (not shown).

In the Athens city center, the daily average value of  $PM_{10} NO_3^-$  concentration is predicted to be  $0.1 \mu g m^{-3}$  by the simulation with the bulk-equilibrium approach (Fig. 9). The dynamic mass-transfer between phases results in a quadrupling of aerosol  $NO_3^-$  at the city center, similar to Capaldo et al. (2000) for Los Angeles. This discrepancy is mainly attributable to the coarse nitrate mass differences and reaches two orders of magnitude. The bulk-equilibrium method predicts slightly higher concentrations of fine nitrate due to the accumulation of the condensing material in the smallest bins, as seen by Capaldo et al. (2000).  $PM_{10-40}$  differences are negligible for nitrate due to low  $PM_{10-40}$  emissions.

## SSA and heterogeneous chemistry in polluted coastal areas

E. Athanasopoulou et al.

Title Page

Abstract

Introduction

Conclusions

References

Tables

Figures

⏪

⏩

◀

▶

Back

Close

Full Screen / Esc

Printer-friendly Version

Interactive Discussion

## 5.4 Local versus regional SSA contribution

The nesting technique is found necessary as the transport of SSA from the boundaries into the nested domain is significant and both temporally and spatially variable during this event. The southern and western boundaries contribute most to total SSA boundary penetration (from  $0.2 \mu\text{g m}^{-3}$  over land to  $23 \mu\text{g m}^{-3}$  over sea), and is found to vary diurnally with the winds. The northern and the eastern boundaries contribute less to total SSA boundary penetration, although higher values are expected to appear during more intense wind regimes over Greece, such as the frequently occurring NE etesian.

## 6 Conclusions

Use of SSA emissions in a simulation of atmospheric chemical dynamics over Greece found that including such emissions led to greater  $\text{PM}_{10}$  levels and allowed investigation of the importance of gas-to-particle conversion in areas with an extended Archipelago. SSA emissions are comparable to all other  $\text{PM}_{10}$  emissions in this case. Over much of the domain, open-ocean emissions contribute most to SSA, but near and over land, surf-zone emissions become important. SSA further impacts  $\text{PM}_{10}$  by reactions with nitric and sulfuric acid, displacing chloride.

A nested approach was used to capture the finer-scale processes (e.g., surf-zone SSA production and near-coastal gas-aerosol interactions), while still simulating a large region. On land, SSA comprised up to 60% of the  $\text{PM}_{10}$  but only 10% of the  $\text{PM}_{2.5}$ , near the coast, decreasing rapidly inland. For example, near the Athens coast (Piraeus port), of the  $18 \mu\text{g m}^{-3}$  total  $\text{PM}_{10}$ ,  $6.5 \mu\text{g m}^{-3}$  was due to SSA emissions. At Thrakomakedones 27 km inland, this dropped to  $1 \mu\text{g m}^{-3}$ .

Nitric and sulfuric acid displacement was found to be important both on-land and over the sea. Interestingly, the highest nitrate levels were found over shipping lanes in the Aegean due to  $\text{NO}_x$  emission oxidation forming  $\text{HNO}_3$ , along with relatively low deposition rates, allowing ample time for the rate-limited mass transfer. The long resi-

Title Page

Abstract

Introduction

Conclusions

References

Tables

Figures

◀

▶

◀

▶

Back

Close

Full Screen / Esc

Printer-friendly Version

Interactive Discussion

dence time of the aerosol nitrate formed over the sea allows this peak to be transported northward towards Athens, and is captured by the nesting procedure. Displacement of  $\text{Cl}^-$  increases  $\text{PM}_{10}$  mass. Use of the finer grid in this region allowed capturing both the surf-zone emissions and relatively rapid chemical dynamics and gas-to-particle conversion near the coast.

While the simulated  $\text{Na}^+$ ,  $\text{Cl}^-$  and  $\text{SO}_4^{2-}$  levels agreed with observations, suggesting the SSA emissions algorithms used are providing reasonable estimates, the simulated nitrate and ammonium levels are low. Summing simulated  $\text{NO}_3^-$  and  $\text{HNO}_3$  (g) found that ample nitrate is formed, but gas-to-particle conversion is underestimated. This is traced to very low levels of total ammonia (ammonium + ammonia), suggesting a low bias in the emissions. Further, comparing the size distribution of simulated nitrate and ammonium to observations provides further evidence it is the lack of ammonium nitrate formation that leads to a low bias in the simulated levels of those two aerosol components.

Examining the size distribution of both SSA emissions and aerosol concentrations shows that SSA mainly affects the coarse mass, thus the adoption of a gas-to-particle mass transfer scheme is necessary. Using a hybrid scheme that combines the equilibrium approach for  $\text{PM}_{2.5}$  with a dynamic approach for coarser particles, led to a quadrupling of aerosol nitrate in the Athens city center versus use of a pure equilibrium approach.

*Acknowledgements.* This research project (PENED) is co-financed by E.U.-European Social Fund (75%) and the Greek Ministry of Development-GSRT (25%). We want to thank the Greek Ministry of the Environment and the HPC-PASECO Company for use of the emission data employed in the study.

---

## SSA and heterogeneous chemistry in polluted coastal areas

E. Athanasopoulou et al.

---

Title Page

Abstract

Introduction

Conclusions

References

Tables

Figures

◀

▶

◀

▶

Back

Close

Full Screen / Esc

Printer-friendly Version

Interactive Discussion

## References

- Aleksandropoulou, V. and Lazaridis, M.: Spatial distribution of gaseous and particulate matter emissions in Greece, *Water, Air, and Soil Pollution*, 153, 1–4, 2004.
- Alexander, B., Park, R. J., Jacob, D. J., Li, Q. B., Yantosca, R. M., Savarino, J., Lee, C. C. W., and Thiemens, M. H.: Sulfate formation in sea-salt aerosols: Constraints from oxygen isotopes, *J. Geophys. Res.*, 110, D10307, doi:10.1029/2004JD005659, 2005.
- Andreas, E. L.: Sea spray and the turbulent air-sea heat fluxes, *J. Geophys. Res.*, 97, 11 429–11 441, 1992.
- Andreas, E.: A New Sea Spray Generation Function for Wind Speeds up to  $32 \text{ m s}^{-1}$ , *J. Phys. Ocean.*, 28(11), 2175–2184, 1998.
- Anthes, R. A. and Warner, T. T.: Development of hydrodynamic models suitable for air pollution and other meteorological studies, *Mon. Weather Rev.*, 106, 1045–1078, 1978.
- Athanasopoulou, E., Bossioli, E., and Tombrou, M.: Modelling of aerosol in the Greater Athens Area, Greece, *Int. J. Environ. Pollut.*, 24, 230–246, 2005.
- Bardouki, H., Liakakou, H., Economou, C., Sciare, J., Smolik, J., Zdimal, V., Eleftheriadis, K., Lazaridis, M., Dye, C., and Mihalopoulos, N.: Chemical composition of size-resolved atmospheric aerosols in the eastern Mediterranean during summer and winter *Atmospheric Environment*, 37, 195–208, 2003.
- Bassett, M. E. and Seinfeld, J. H.: Atmospheric equilibrium model of sulfate and nitrate aerosol, *Atmos. Environ.*, 17, 2237–2252, 1983.
- Bassett, M. E. and Seinfeld, J. H.: Atmospheric equilibrium model of sulfate and nitrate aerosol. II, Particle size analysis, *Atmos. Environ.*, 18, 1163–1170, 1984.
- Bessagnet, B., Hodzic, A., Vautard, R., Beekmann, M., Cheinet, S., Honore, C., Liousse, C., and Rouil, L.: Aerosol modeling with CHIMERE—preliminary evaluation at the continental scale, *Atmos. Environ.*, 38, 2803–2817, 2004.
- Binkowski, F. S. and Shankar, U.: The regional particulate matter model, 1: model description and preliminary results, *J. Geophys. Res.*, 100, 26 191–26 209, 1995.
- Blanchard, D. C.: The electrification of the atmosphere by particles from bubbles in the sea, in: *Progr. Oceanogr.*, edited by: M. Sears, 73–202, Pergamon Press, New York, 1963.
- Bortkovskii, R. S.: Air-Sea exchange of heat and moisture during storms, 194 pp., D. Reidel Publishing company, Dordrecht, 1987.
- Bossioli, E., Tombrou, M., and Pilinis, C.: Adapting the Speciation of the VOCs Emission Inven-

ACPD

8, 3807–3841, 2008

### SSA and heterogeneous chemistry in polluted coastal areas

E. Athanasopoulou et al.

Title Page

Abstract

Introduction

Conclusions

References

Tables

Figures

◀

▶

◀

▶

Back

Close

Full Screen / Esc

Printer-friendly Version

Interactive Discussion

- tory, in the Greater Athens Area, *Water, Air, Soil Pollut.: Focus*, 2(5–6), 141–153, 2002.
- Byun, D. W., Pleim, J., Tang, R., and Bourgeois, A.: Meteorology-chemistry interface processor (MCIP) for Models-3 Community Multiscale Air Quality (CMAQ) modeling system. In *Science Algorithms of the EPA Models-3 Community Multiscale Air Quality (CMAQ) Modeling System. Part II: Chapters 9–18*, edited by: D. W. Byun, and J. K. S. Ching, EPA-600/R-99/030, National Exposure Research Laboratory, U.S. Environmental Protection Agency, Research Triangle Park, NC, 12-1–12-86, 1999.
- Capaldo, K. P., Pilinis, C., and Pandis, S. P.: A computationally efficient hybrid approach for dynamic gas/aerosol transfer in air quality models, *Atmos. Environ.*, 34, 3617–3627, 2000.
- Chang, J. S., Brost, R. A., Isaksen, I. S. A., Madronich, S., Middleton, P., Stockwell, W. R., and Walcek, C. J.: A three-dimensional Eulerian Acid Deposition Model: Physical concepts and formulation, *J. Geophys. Res.*, 92, 14 681–14 700, 1987.
- Clarke, A. D., Owens, S. R., and Zhou, J.: An ultrafine sea-salt flux from breaking waves: Implications for cloud condensation nuclei in the remote marine atmosphere, *J. Geophys. Res.*, 111, D06202, doi:10.1029/2005JD006565, 2006.
- Dandou A., Tombrou, M., Akylas, E., Soulakellis, N., and Bossioli, E.: Development and evaluation of an urban parameterization scheme in the Penn State/NCAR Mesoscale Model (MM5), *J. Geophys. Res.-Atmos.*, 110, D10102, doi:10.1029/2004JD005192, 2005.
- De Leeuw, G., Neele, F. P., Hill, M., Smith, M. H. and Vignati, E.: Production of sea spray aerosol in the surf zone, *Journal of Geophysical Research*, 105(D24), 29 397–29 410, 2000.
- Eleftheriadis, K., Balis, D., Ziomas, I., Colbeck, I., and Manalis, N.: Atmospheric aerosol and gaseous species in Athens, Greece', *Atmos. Environ.*, 32, 2183–2191, 1998a.
- Eleftheriadis, K., Chung, M. C., and Colbeck, I.: Atmospheric aerosol formation over Athens, *J. Aerosol Science*, 29, S25-6, 1998b.
- Eleftheriadis, K., Chung, M., Michaleas, S., and Colbeck, I.: Atmospheric aerosol evolution and transport over Athens, In: Th. Lekkas (Ed.), *Proceedings of the Sixth Conference on Environmental Science and Technology*, 30 August–2 September 1999, Samos, Greece, Vol. A, University of the Aegean, 137–144, 1999.
- Eleftheriadis, K., Colbeck, I., Housiadas, C., Lazaridis, M., Mihalopoulos, N., Mitsakou, C., Smolík, J., and Ždimal, V.: Size distribution, composition and origin of the submicron aerosol in the marine boundary layer during the eastern Mediterranean “SUB-AERO” experiment, *Atmos. Environ.*, 40(32), 6245–6260, 2006.
- EMPA: Anteil des Strassenverkehrs an den  $PM_{10}$  und  $PM_{2.5}$  Immissionen. NFP41, Verkehr und

---

**SSA and  
heterogeneous  
chemistry in polluted  
coastal areas**E. Athanasopoulou et al.

---

Title Page

Abstract

Introduction

Conclusions

References

Tables

Figures

◀

▶

◀

▶

Back

Close

Full Screen / Esc

Printer-friendly Version

Interactive Discussion

---

**SSA and  
heterogeneous  
chemistry in polluted  
coastal areas**E. Athanasopoulou et al.

---

Title Page

Abstract

Introduction

Conclusions

References

Tables

Figures

◀

▶

◀

▶

Back

Close

Full Screen / Esc

Printer-friendly Version

Interactive Discussion

Umwelt, Dübendorf, Switzerland, 2000.

Environ: User's guide to the comprehensive air quality model with extensions (CAMx), version 4.10s, report, ENVIRON Int. Corp., Novato, Calif., available at <http://www.camx.com>, 2004.

5 Fairall, C. W., Davidson, K. L., and Schacher, G. E.: An analysis of the surface production of sea-salt aerosols, *Tellus*, 35B, 31–39, 1983.

Foltescu, V. L., Pryor, S. C., and Bennet, C.: Sea salt generation, dispersion and removal on the regional scale, *Atmos. Environ.*, 39, 2123–2133, 2004.

Fountoukis, C. and Nenes, A.: ISORROPIA II: a computationally efficient thermodynamic equilibrium model for  $K^+$ – $Ca^{2+}$ – $Mg^{2+}$ – $NH_4^+$ – $Na^+$ – $SO_4^{2-}$ – $NO_3^-$ – $Cl^-$ – $H_2O$  aerosols, *Atmos. Chem. Phys.*, 7, 4639–4659, 2007,  
<http://www.atmos-chem-phys.net/7/4639/2007/>.

Gathman, S. G.: A time-dependent oceanic aerosol profile model, NRL Report 8536, 35, Naval Research Laboratory, Washington, DC, 1982.

15 Gery, M. W., Whitten, G. Z., Killus, J. P., and Dodge, M. C.: A photochemical kinetics mechanism for urban and regional scale computer modeling, *J. Geophys. Res.*, 94, 12 925–12 956, 1989.

Gong S. L.: A parameterization of sea-salt aerosol source function for sub- and super-micron particles', *Global Biogeochemical Cycles*, Vol. 17(4), pp. (8)-1–(8)-6, 2003.

20 Gong, S. L., Barrie, L. A., and Blanchet, J.-P: Modeling sea-salt aerosols in the atmosphere 1. Model development, *Journal of geophysical research*, 102(D3), 3805–3818, 1997.

Hien, P. D., Bac, V. T., and Thinh, N. T. H.: Investigation of sulfate and nitrate formation on mineral dust particles by receptor modeling, *Atmos. Environ.*, 39, 7231–7239, 2005.

25 Hodzic, A., Bessagnet, B., and Vautard, R.: A model evaluation of coarse-mode nitrate heterogeneous formation on dust particles, *Atmos. Environ.*, 40(22), 4158–4171, 2006.

Hoppel, W. A., Frick, G. M., and Fitzgerald, J. W.: Surface source function for sea-salt aerosol and aerosol dry deposition to the ocean surface, *J. Geophys. Res.*, 107, 1–17, 2002.

Iida, N., Toba, Y., and Chaen, M.: A new expression for the production rate of sea water droplets on the sea surface, *J. Oceanography*, 48(4), 439–460, 1992.

30 Kassomenos, P., Flocas, H. A., Lykoudis, S., and Petrakis, M.: Analysis of mesoscale patterns in relation to synoptic conditions over an urban Mediterranean basin, *Theor. Appl. Climatol.*, 59, 215–229, 1998.

Koo, B., Gaydos, T. M., and Pandis, S. N.: Evaluation of the equilibrium, hybrid, and dynamic

---

**SSA and  
heterogeneous  
chemistry in polluted  
coastal areas**

---

E. Athanasopoulou et al.

---

[Title Page](#)[Abstract](#)[Introduction](#)[Conclusions](#)[References](#)[Tables](#)[Figures](#)[⏪](#)[⏩](#)[◀](#)[▶](#)[Back](#)[Close](#)[Full Screen / Esc](#)[Printer-friendly Version](#)[Interactive Discussion](#)

aerosol modeling approaches, *Aerosol Sci. Tech.*, 37, 53–64, 2003.

Lazaridis, M., Eleftheriadis, K., Smolik, J., Colbeck, I., Kallos, G., Drossinos, Y., Zdimas, V., Vecera, Z., Mihalopoulos, N., Mikuska, P., Bryant, C., Housiadas, C., Spyridaki, A., Astitha, M., and Havranek, V.: Dynamics of fine particles and photo-oxidants in the Eastern Mediterranean (SUB-AERO), *Atmos. Environ.*, 40, 6214–6228, 2006.

Lewis, E. R. and Schwartz, S. E.: *Sea Salt Aerosol Production: Mechanisms, Methods, Measurements, and Models: A Critical Review*, American Geophysical Union, Washington, DC, 2004.

Lewis, E. R. and Schwartz, S. E.: Comment on “size distribution of sea-salt emissions as a function of relative humidity”, *Atmos. Environ.*, 40, 588–590, 2006

Ling, S. C., Kao, T. W., and Saad, A. I.: Microdroplets and transport of moisture from ocean, *J. Eng. Mech. Div.*, 106, 1327–1339, 1980.

Lurmann, F. W., Wexler, A. S., Pandis, S. N., Musarra, S., Kumar, N., and Seinfeld, J. H.: Modeling urban and regional aerosols-II, Application to California’s south coast air basin, *Atmos. Environ.*, 31, 2695–2715, 1997.

Martensson, E. M., Nilsson, E. D., De Leeuw, G., Cohen, L. H., and Hansson, H.-C.: Laboratory simulations and parameterization of the primary marine aerosol production, *J. Geophys. Res.*, 108, 1081–12, 2003.

Mebust, M. R., Eder, B. K., Binkowski, F. S., and Roselle, S. J.: Models-3 Community Multi-scale Air Quality (CMAQ) model aerosol component. 2. Model evaluation, *J. Geophys. Res.* 108(D6), 4184, doi:10.1029/2001JD001410, 2003.

Melas, D., Ziomas, I., Klemm, O., and Zerefos, C. S.: Anatomy of the sea-breeze circulation in Athens area under weak largescale ambient winds, *Atmos. Environ.*, 32(12), 2223–2237, 1998.

Meng, Z. and Seinfeld, J. H.: Timescales to achieve atmospheric gas-aerosol equilibrium for volatile species, *Atmos. Environ.*, 30, 2889–2900, 1996.

Monahan, E. C.: *Coastal Aerosol Workshop Proceedings*, edited by: A. K. Goroch and G. L. Geernaert, Rep. NRL/MR/7542-95-7219, 138 pp., Nav. Res. Lab., Monterey, Calif., 1995.

Monahan, E. C., Spiel, D. E., and Davidson, K. L.: A model of marine aerosol generation via whitecaps and wave disruption, in *Oceanic Whitecaps*, edited by: E. Monahan and G. M. Niocaill, 167–174, D. Reidel, Norwell, Mass, 1986.

Nenes, A., Pilinis, C., and Pandis, S. N.: ISORROPIA: a new thermodynamic equilibrium model for multiphase multicomponent marine aerosols, *Aquat. Geochem.*, 4, 123–52, 1998.

**SSA and  
heterogeneous  
chemistry in polluted  
coastal areas**

E. Athanasopoulou et al.

Title Page

Abstract

Introduction

Conclusions

References

Tables

Figures

◀

▶

◀

▶

Back

Close

Full Screen / Esc

Printer-friendly Version

Interactive Discussion

- O'Brien, J.: A Note on the Vertical Structure of the Eddy Exchange Coefficient in the Planetary Boundary Layer, *J. Atmos. Sci.*, 27(8), 1213–1215, 1970.
- O'Dowd, C., Smith, M. H., Ian, C. E. and Jason, L. A.: Marine Aerosol, Sea-Salt, And The Marine Sulphur Cycle: A Short Review, *Atmos. Environ.* 31, 1, 73–80, 1997.
- 5 Pierce, J. R. and Adams, P. J.: Global evaluation of CCN formation by direct emission of sea salt and growth of ultrafine sea salt, *J. Geophys. Res.*, 111, 2006.
- Russell, A. G. and Cass, G.: Verification Of A Mathematical Model For Aerosol Nitrate And Nitric Acid Formation And Its Use For Control Measure Evaluation, *Atmos. Environ.*, 20, 2011–2025. 1986.
- 10 Salvador, P., Begoña, A., Xavier, Q., Andrés A., and Miguel, C.: Characterisation of local and external contributions of atmospheric particulate matter at a background coastal site, *Atmos. Environ.*, 41, 1–17, 2007.
- Saxena, P., Seigneur, C., Hudischewskyj, A. B., and Seinfeld, J. H.: A comparative study of equilibrium approaches to the chemical characterizations of secondary aerosols, *Atmos. Environ.*, 20, 1471–1484, 1986.
- 15 Scheff, P. A. and Valiozis, C.: Characterization and source identification of respirable particulate matter in Athens, Greece, *Atmos. Environ.*, 24(A1), 203–211, 1990.
- Seinfeld, J. H. and Pandis, S. P.: *Atmospheric chemistry and physics – from air pollution to climate change*, John Wiley & Sons, Inc, 1998.
- 20 Siskos, P. A., Bakeas, E. B., Lioli, I., Smirnioudi, V. N., and Koutrakis, P.: Chemical characterization of PM<sub>2.5</sub> aerosols in Athens-Greece, *Environ. Technol.*, 22, 687–695, 2001.
- Smith, M. H. and Harrison, N. M.: The Sea Spray Generation Function, *J. Atmos. Sci.*, 29, 189–190, 1998.
- Smith, M. H., Park, P. M., and Consterdine, I. E.: Marine aerosol concentrations and estimated fluxes over the sea, *Quart. J. Roy. Meteorol. Soc.*, 119, 809–824, 1993.
- 25 Smolik, J., Zdimal, V., Schwarz, J., Lazaridis, M., Havranek, V., Eleftheriadis, K., Mihalopoulos, N., Bryant, C., and Colbeck, I.: Size resolved mass concentration and elemental composition of atmospheric aerosols over the Eastern Mediterranean area, *Atmos. Chem. Phys.*, 3, 2207–221, 2003,
- 30 <http://www.atmos-chem-phys.net/3/2207/2003/>.
- Sotiropoulou, R. E. P., Tagaris, E., and Pilinis, C.: An estimation of the spatial distribution of agricultural ammonia emissions in the Greater Athens Area, *The Science Of The Total Environment*, 318, 159–69, 2003.

---

**SSA and  
heterogeneous  
chemistry in polluted  
coastal areas**

---

E. Athanasopoulou et al.

---

[Title Page](#)[Abstract](#)[Introduction](#)[Conclusions](#)[References](#)[Tables](#)[Figures](#)[⏪](#)[⏩](#)[◀](#)[▶](#)[Back](#)[Close](#)[Full Screen / Esc](#)[Printer-friendly Version](#)[Interactive Discussion](#)

- Spyridaki, A., Lazaridis, M., Eleftheriadis, K., Smolik, J., Mihalopoulos, N., and Aleksandropoulou, V.: Modelling and evaluation of size-resolved aerosol characteristics in the Eastern Mediterranean during the SUB-AERO project, *Atmos. Environ.*, 40, 6261–6275, 2006.
- 5 Strader R., Gurciullo, C., Pandis, S. N., Kumar, N., and Lurmann, F. W.: Development of gas-phase chemistry, secondary organic aerosol, and aqueous-phase chemistry modules for PM modelling, Final report for CRC Project A21-1 prepared for the Coordinating Research Council, Atlanta, GA by Sonoma Technology, Inc. Petaluma, CA, STI-97510-1822-FR, October, 1998.
- Torfs, K. and Grieken, van R.: Chemical relations between atmospheric aerosols, deposition and stone decay layers on historic buildings at the Mediterranean coast, in: *Atmos. Environ.*, 31, 2179–2192, 1997.
- 10 Tsitouridou, R., Voutsas, D., and Kouimtzi, T.: Ionic composition of PM10 in the area of Thessaloniki, Greece, *Chemosphere*, 52, 883–891, 2003.
- Vignati, E., de Leeuw, G., and Berkowicz, R.: Modeling coastal aerosol transport and effects of surf-produced aerosols on processes in the marine atmospheric boundary layer, *J. Geophys. Res.*, 106(d17), 20 225–20 238, 2001.
- 15 Wall, S. M., John, W., and Ondo, J. L.: Measurement of aerosol size distributions for nitrate and major ionic species, *Atmos. Environ.*, 22, 1649–1656, 1988.
- Witek, M. L., Flatau, P. J., Quinn, P. K., and Westphal, D. L.: Global sea-salt modeling: Results and validation against multicampaign shipboard measurements, *J. Geophys. Res.*, 112, D08115, doi:10.1029/2006JD007779, 2007.
- 20 Woodcock, A. H., Blanchard, D. C., and Rooth, C. G. H.: Salt-induced convection and clouds, *J. Atmos. Sci.*, 20, 159–169, 1963.
- Woolf, D. K., Monahan, E. C., and Spiel, D. E.: Quantification of the marine aerosol produced by whitecaps, in *Seventh Congress on Ocean-Atmosphere Interaction*, 182–185, Am. Meteorol. Soc., Anaheim, CA, 1988.
- 25 Wu, J.: Bubble flux and marine aerosol spectra under various wind velocities, *J. Geophys. Res.*, 97(C2), 2327–2333, 1992.
- Wu, J.: Production of spume drops by the wind tearing of wave crests: the search for quantification, *J. Geophys. Res.*, 98(C10), 18 221–18 227, 1993.
- 30 Zhang, K. M., Knipping, M. E., Wexler, A. S., Bhawe, P. V., and Tonnesen, S. G.: Size distribution of sea-salt emissions as a functions of relative humidity, *Atmos. Environ.*, 39, 3373–3379, 2005a.

Zhang, K. M., Knipping, M. E., Wexler, A. S., Bhave, P. V., and Tonnesen, S. G.: Reply to comment on “Size distribution of sea-salt emissions as a function of relative humidity”, *Atmos. Environ.*, 40(3), 591–592, 2005b.

5 Zhang, Y., Seigneur, C., Seinfeld, J. H., Jacobson, M., Clegg, S. L., and Binkowski, F. S.: A comparative review of inorganic aerosol thermodynamic equilibrium modules: similarities, differences, and their likely causes, *Atmos. Environ.*, 34, 117–37, 2000.

Ziomas, I., Melas, D., Zerefos, C. S., Bais, A. F., and Paliatsos, A. G.: Forecasting peak pollutant levels from meteorological variables, *Atmos. Environ.*, 29, 3703–3711, 1995.

ACPD

8, 3807–3841, 2008

---

**SSA and  
heterogeneous  
chemistry in polluted  
coastal areas**

E. Athanasopoulou et al.

---

Title Page

Abstract

Introduction

Conclusions

References

Tables

Figures

⏪

⏩

◀

▶

Back

Close

Full Screen / Esc

Printer-friendly Version

Interactive Discussion

**Table 1.** SSA source functions and parameters employed by this study.

Emission rates M (g m <sup>-2</sup> s <sup>-1</sup> )	
$M_{\text{Open-ocean}} = M_{\text{CL06}} + M_{\text{G-M03}}$	$M_{\text{Surf-zone}} = M_{\text{DEL00}}$
$M_{\text{CL06}} = \sum_{i=1}^3 \int_{r_{i-1}/C_{80}}^{r_i/C_{80}} \frac{dM_{\text{CL06}_i}}{dr_{\text{RH}}}$	$M_{\text{G-M03}} = \int_{r_5/C_{80}}^{r_4/C_{80}} \frac{dM_{\text{G-M03}}}{dr_{\text{RH}}}$
$\frac{dM_{\text{CL06}_i}}{dr_{\text{RH}}} = 10^4 \frac{3.84 \cdot 10^{-6} U_{10}^{3.41}}{\ln 10 \cdot r_{\text{RH}}} A_i \cdot NM$	$\frac{dM_{\text{DEL00}}}{dr_{\text{RH}}} = NM \cdot 1.1 \cdot 10^7 e^{0.23 U_{10} (2r_{\text{RH}} C_0)^{-1.65}}$
$\frac{dM_{\text{G-M03}}}{dr_{\text{RH}}} = C_{80} \cdot NM \cdot 1.373 U_{10}^{3.41} r_{\text{RH}}^{-A_4} \cdot (1 + 0.057 r_{\text{RH}}^{3.45}) \cdot 10^{1.607 e^{-B^2}}$	
$C_{80} = 1.82 \left( \frac{1 - RH}{2 - RH} \right)^{1/3}$	$NM = 10^{-15} \pi \frac{8r_{\text{RH}}^3}{6} \rho x$
$A_1 = -7.502^3 + 1.212^6 r_{\text{RH}} C_{80}^-$	$A_2 = 5.781^3 + 1.753^4 r_{\text{RH}} C_{80}^-$
$2.971^7 (r_{\text{RH}} C_{80})^2 + 3.283^8 (r_{\text{RH}} C_{80})^3 -$	$9.858^4 (r_{\text{RH}} C_{80})^2 + 1.505^5 (r_{\text{RH}} C_{80})^3 -$
$1.716^9 (r_{\text{RH}} C_{80})^4 + 3.435^9 (r_{\text{RH}} C_{80})^5$	$9.61^4 (r_{\text{RH}} C_{80})^4 + 2.24^4 (r_{\text{RH}} C_{80})^5$
$A_3 = 6.474^2 + 1.259^3 r_{\text{RH}} C_{80}^-$	$A_4 = 4.7 (1 + \Theta \cdot r_{\text{RH}})^{-0.017 r_{\text{RH}}^{-1.44}}, \quad \Theta = 30$
$8.092^2 (r_{\text{RH}} C_{80})^2 + 1.828^2 (r_{\text{RH}} C_{80})^3 -$	
$1.82 (r_{\text{RH}} C_{80})^4 + 6.771^{-1} (r_{\text{RH}} C_{80})^5$	$B = \frac{0.433 - \log r_{\text{RH}}}{0.433}$
$r_{\text{RH}}$ =particle radius at local/ambient RH, $r_0=0.005$ , $r_1=0.065$ , $r_2=0.6$ , $r_3=4$ , $r_4=10(\mu\text{m})$ .	
$x=3.1657-19.079RH+55.72RH^2-83.998RH^3+63.436RH^4-19.248RH^5$ .	
$\rho=1000(3.8033-16.248RH+46.085RH^2-68.317RH^3+50.932RH^4-15.261RH^5)$ (kg m <sup>-3</sup> )	

## SSA and heterogeneous chemistry in polluted coastal areas

E. Athanasopoulou et al.

Title Page

Abstract

Introduction

Conclusions

References

Tables

Figures

◀

▶

◀

▶

Back

Close

Full Screen / Esc

Printer-friendly Version

Interactive Discussion

**Table 2.** Inorganic aerosol species concentrations ( $\mu\text{g m}^{-3}$ ) observed during other studies with similar conditions. Data in parentheses show either minimum and maximum values (2 numbers) or the standard deviation of the average value (1 number).

Location	Time period	$\text{Cl}^-$	$\text{Na}^+$	$\text{SO}_4^{=}$	$\text{NO}_3^-$	$\text{NH}_4^+$	Wind ( $\text{m s}^{-1}$ )	Reference
Athens	1995 <sup>1#</sup>	3.1	2.4	10.6	2.5	2.2	SE-SW	Siskos et al., 2001
	15/04-12/06/1987 <sup>1</sup>	0.3 (0–1.3)	0.4 (0–0.2)	10.4 (4–24)	2 (0.5–5)	–	2 (0.3–10.3)	Scheff and Valiozis, 1990
	29/08-16/09/1994 <sup>*#</sup>	0.5	0.5	5.5 (3–10)	2 (1–5)	1.5 (0.5–4)	(1–14)	Eleftheriadis et al., 1998a
Piraeus (Castella)	17/07-06/08/1997 <sup>*#</sup>	0.3	0.7	4	1.5	2.5	–	Eleftheriadis et al., 1998b
Ag. Stefanos		0.5	1	8	3	3.5	–	
Eleusis	2-year period <sup>2</sup>	4 (3.7)	1.6 (0.6)	8 (9.3)	3.1 (3.2)	–	–	Torfs and Grieken, 1997
Thessaloniki	07/1997-07/1998 <sup>3</sup>	0.9 (0.5)	0.6 (0.6)	4.8 (2)	2.8 (1.4.)	2.7 (1.6)	–	Tsitouridou et al., 2003
		1.4 (0.8)	0.6 (0.5)	7.2 (5.8)	3.4 (1.9)	3.5 (2.3)	–	
		1 (0.7)	1 (1.1)	7.3 (5.8)	4 (2.1)	4.2 (3.2)	–	
Aegean sea	25–29/07/2000 <sup>*</sup>	0.01 (0.1)	0.1 (0.1)	10.1 (1.1)	0.2 (0.0)	7.2 (2.9)	3.7	Eleftheriadis et al., 2006
	25–30/07/2000 <sup>*</sup>	2.0	–	8.5	2.9	1.5	–	Lazaridis et al., 2006
	26–29/07/2000 <sup>3</sup>	0.6	0.8	9.3	3.2	5.7	–	Smolik et al., 2003
Finokalia	13–16/07/2000 <sup>3</sup>	3.1	4.1	4.2	3.4	1.0	–	
	26–30/07/2000 <sup>3</sup>	0.2	0.6	8.2	2.0	3.7	–	
	10–31/07/2000 <sup>4</sup>	2.3 (0.4)	2 (0.3)	6.9 (0.9)	2.75 (0.41)	2.4	– (0.4)	Lazaridis et al., 2006; Bardouki et al., 2003
	25–29/07/2000 <sup>*</sup>	0.1 (0.1)	0.1 (0.0)	6.9 (1.7)	0.27 (0.09)	3.7 (0.7)	3.7	Eleftheriadis et al., 2006

<sup>1</sup> Average ion concentration in  $\text{PM}_{2.5}$  mass; <sup>2</sup> in  $\text{PM}_2$  mass; <sup>3</sup> in  $\text{PM}_{10}$  mass; <sup>4</sup> in  $\text{PM}_{15}$  mass.

\* Unidentified fraction of aerosol mass measured; # Rough mean approximations from data shown in figure plots.

**SSA and  
heterogeneous  
chemistry in polluted  
coastal areas**

E. Athanasopoulou et al.

Title Page

Abstract

Introduction

Conclusions

References

Tables

Figures

◀

▶

◀

▶

Back

Close

Full Screen / Esc

Printer-friendly Version

Interactive Discussion

**SSA and  
heterogeneous  
chemistry in polluted  
coastal areas**

E. Athanasopoulou et al.

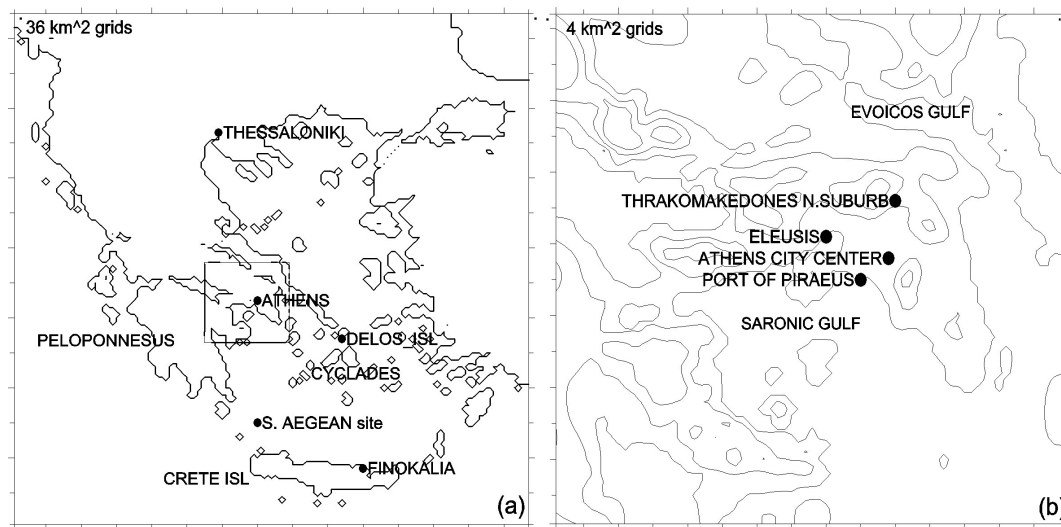


**Fig. 1.** Application domain and monitoring stations: **(a)** the parent domain (covers Greece, with outside ticks at 60 km intervals and **(b)** the nested domain (embedded rectangle) covers the Attica peninsula, with outside ticks at 10 km. Topography contours at 300 m intervals.

[Title Page](#)[Abstract](#)[Introduction](#)[Conclusions](#)[References](#)[Tables](#)[Figures](#)[◀](#)[▶](#)[◀](#)[▶](#)[Back](#)[Close](#)[Full Screen / Esc](#)[Printer-friendly Version](#)[Interactive Discussion](#)

**SSA and  
heterogeneous  
chemistry in polluted  
coastal areas**

E. Athanasopoulou et al.

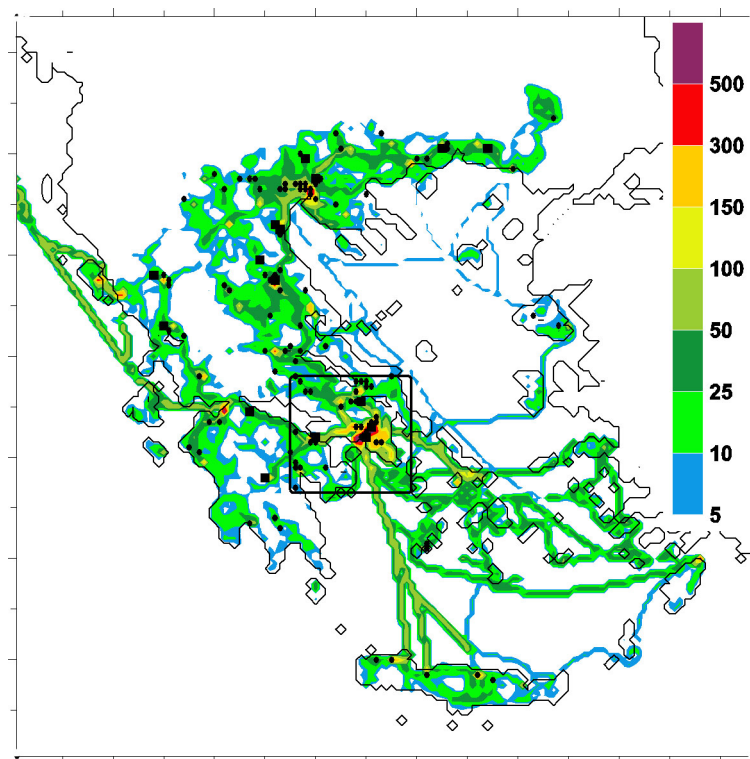


**Fig. 2.** Spatial distribution of the daily average NO<sub>x</sub> emission rates (kg cell<sup>-1</sup> hr<sup>-1</sup>) over Greece, during summer. Solid rectangles show point source emissions greater than 500 kg hr<sup>-1</sup> and circles are the rest industrial sources.

[Title Page](#)[Abstract](#)[Introduction](#)[Conclusions](#)[References](#)[Tables](#)[Figures](#)[◀](#)[▶](#)[◀](#)[▶](#)[Back](#)[Close](#)[Full Screen / Esc](#)[Printer-friendly Version](#)[Interactive Discussion](#)

## SSA and heterogeneous chemistry in polluted coastal areas

E. Athanasopoulou et al.

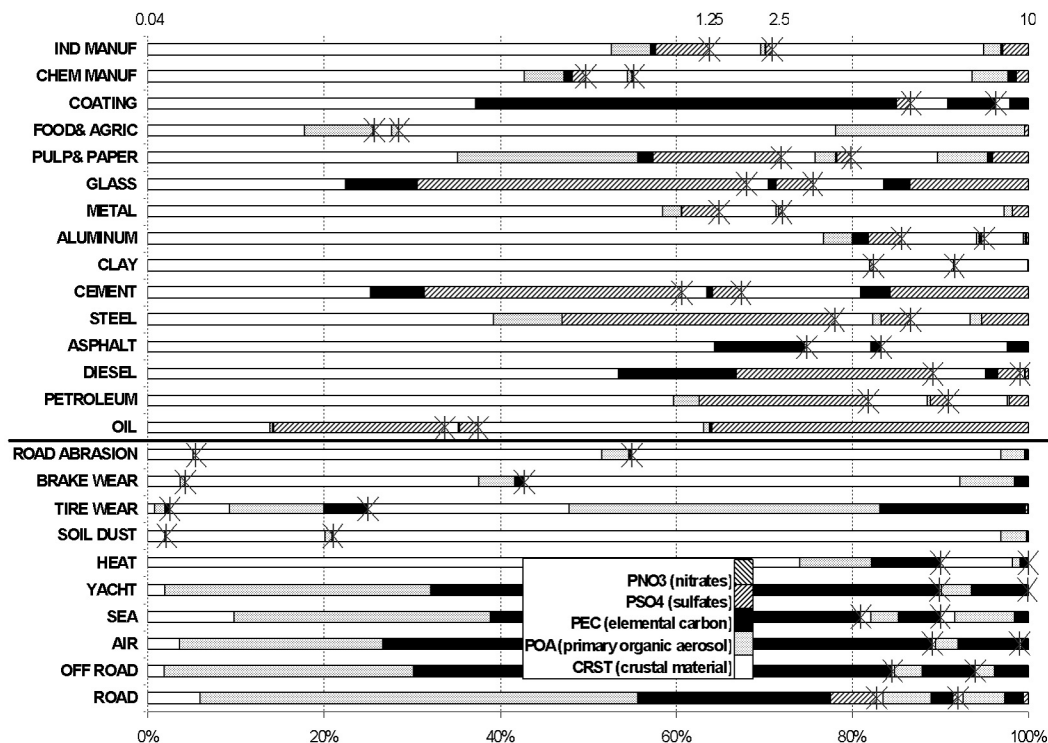


**Fig. 3.** Speciation profiles of  $PM_{10}$  emissions from the main area (lower section) and point (upper section) sources. Crosses define the main size sections of  $PM_{10}$  speciation. Their cutoff diameters ( $\mu m$ ) are shown on top.

Title Page

Abstract

Introduction

Conclusions

References

Tables

Figures

◀

▶

◀

▶

Back

Close

Full Screen / Esc

Printer-friendly Version

Interactive Discussion

**SSA and  
heterogeneous  
chemistry in polluted  
coastal areas**

E. Athanasopoulou et al.

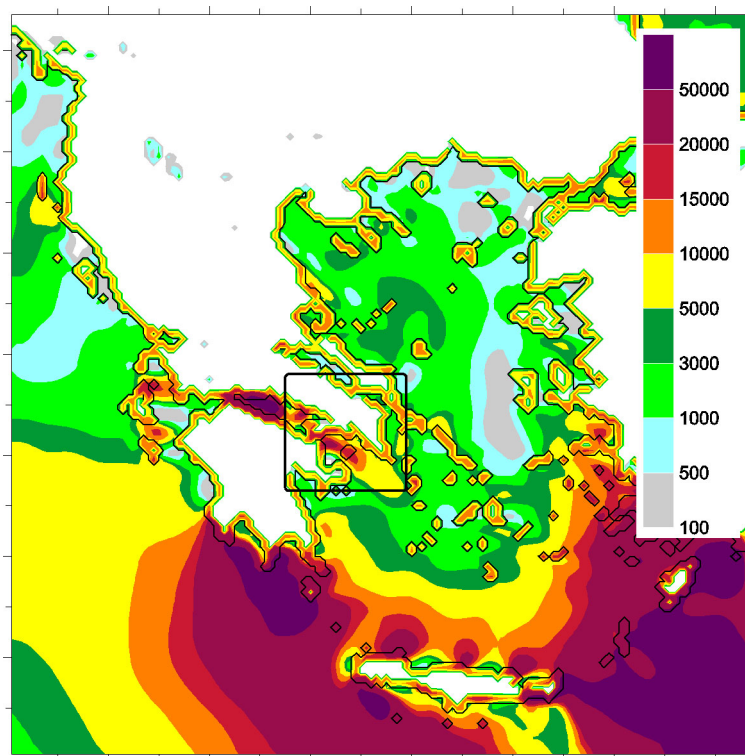


**Fig. 4.** Spatial distribution of the daily average SSA emission rates ( $\text{g cell}^{-1} \text{hr}^{-1}$ ) over Greece. The SSA emissions are distributed uniformly over the coastal computational cells.

[Title Page](#)[Abstract](#)[Introduction](#)[Conclusions](#)[References](#)[Tables](#)[Figures](#)[◀](#)[▶](#)[◀](#)[▶](#)[Back](#)[Close](#)[Full Screen / Esc](#)[Printer-friendly Version](#)[Interactive Discussion](#)

## SSA and heterogeneous chemistry in polluted coastal areas

E. Athanasopoulou et al.

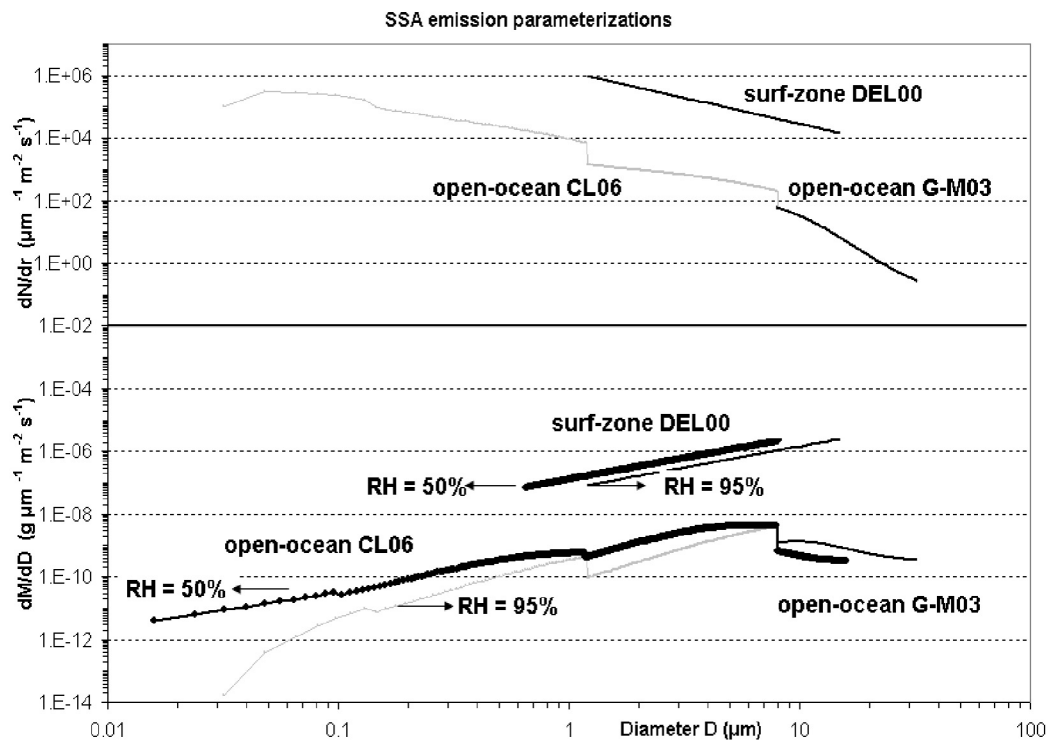


**Fig. 5.** Sea-salt number ( $N$ , upper part) and mass ( $M$ , lower part) fluxes as a function of particle size calculated from the applied source functions ( $U_{10}=13\text{ m s}^{-1}$ ), which are shown near the curves. RH ranges from 50 (thick lines) to 95% (thin lines) over the marine area of Greece.

Title Page

Abstract

Introduction

Conclusions

References

Tables

Figures

◀

▶

◀

▶

Back

Close

Full Screen / Esc

Printer-friendly Version

Interactive Discussion

**SSA and  
heterogeneous  
chemistry in polluted  
coastal areas**

E. Athanasopoulou et al.

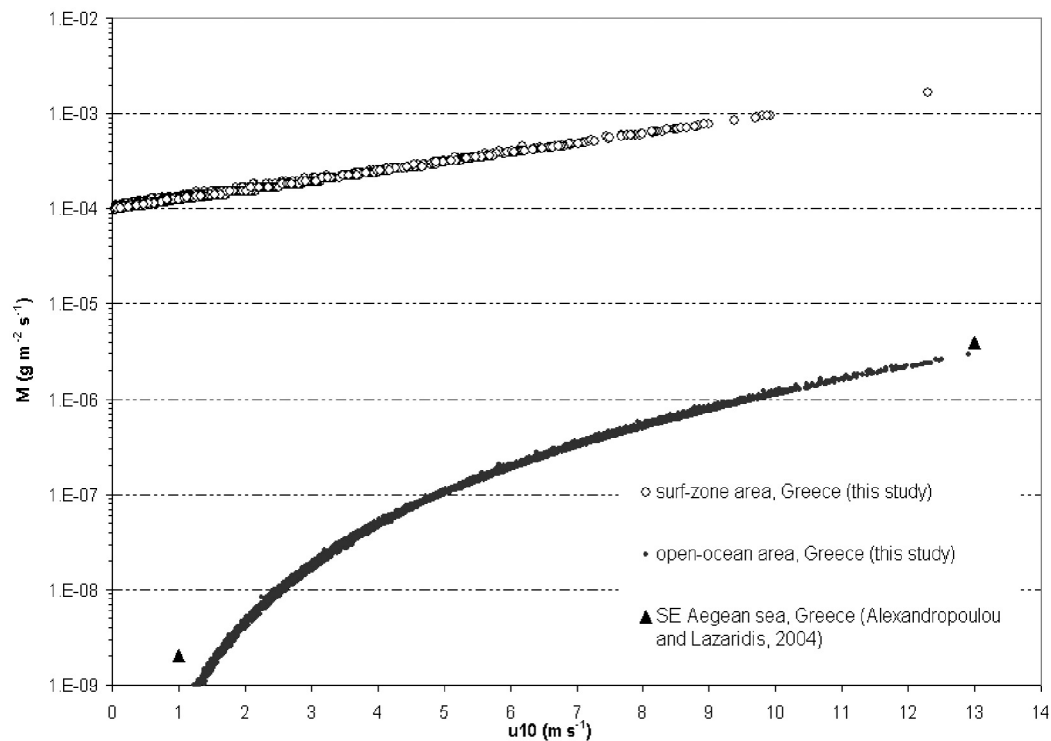


**Fig. 6.** Wind dependence of SSA emissions, calculated for open-ocean and surf-zone areas.

[Title Page](#)[Abstract](#)[Introduction](#)[Conclusions](#)[References](#)[Tables](#)[Figures](#)[◀](#)[▶](#)[◀](#)[▶](#)[Back](#)[Close](#)[Full Screen / Esc](#)[Printer-friendly Version](#)[Interactive Discussion](#)

SSA and  
heterogeneous  
chemistry in polluted  
coastal areas

E. Athanasopoulou et al.

Title Page

Abstract

Introduction

Conclusions

References

Tables

Figures

◀

▶

◀

▶

Back

Close

Full Screen / Esc

Printer-friendly Version

Interactive Discussion

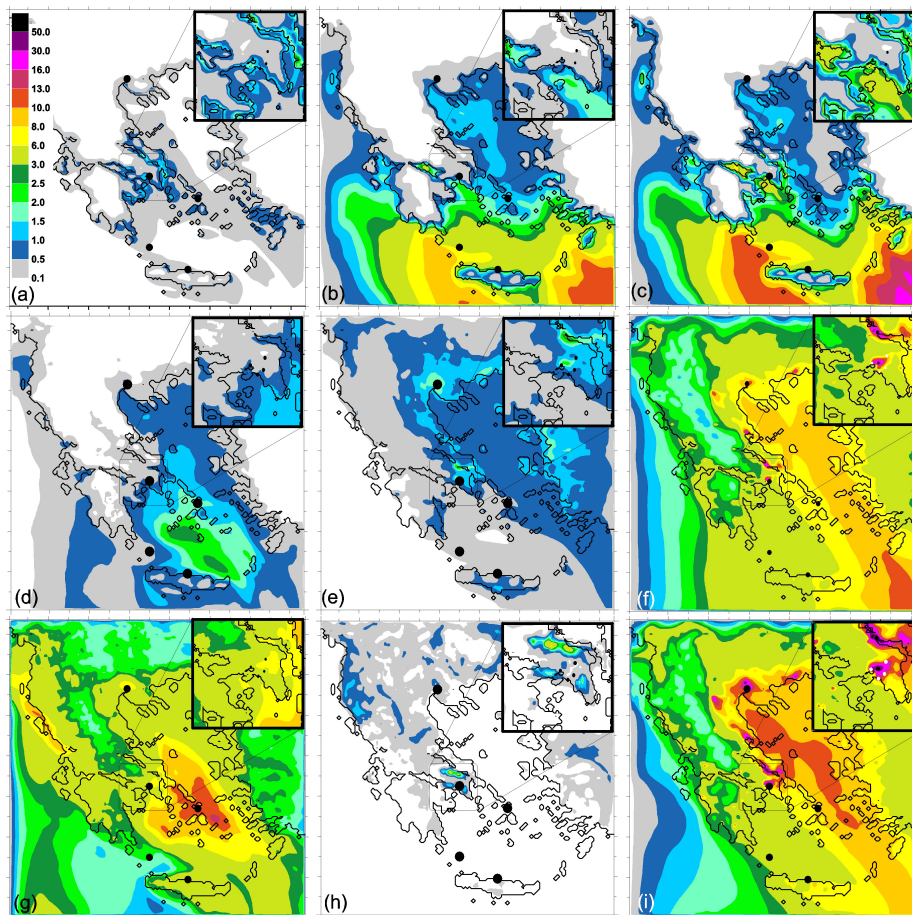


**Fig. 7.** Spatial distribution of average daily  $\text{PM}_{10}$  species concentrations ( $\mu\text{g m}^{-3}$ ) over Greece: **(a)** surf-zone sodium ( $\text{Na}^+$ ), **(b)** open-ocean  $\text{Na}^+$ , **(c)** chloride ( $\text{Cl}^-$ ), **(d)** nitrate ( $\text{NO}_3^-$ ), **(e)** ammonium ( $\text{NH}_4^+$ ), **(f)** sulfate ( $\text{SO}_4^{2-}$ ), **(g)** nitric acid ( $\text{HNO}_3$ ), **(h)** ammonia ( $\text{NH}_3$ ), **(i)** non-SSA  $\text{PM}_{10}$ .

## SSA and heterogeneous chemistry in polluted coastal areas

E. Athanasopoulou et al.

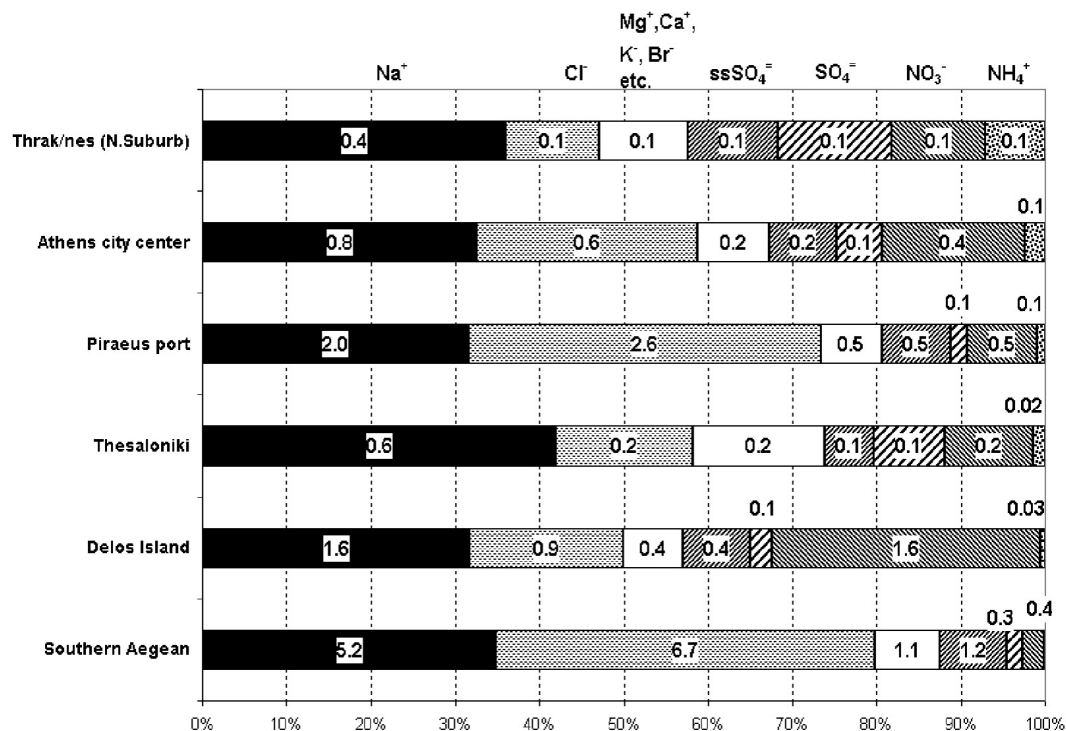


**Fig. 8.** Chemical speciation of the SSA-derived in the PM<sub>10</sub> concentrations at the selected sites. Chemical species are shown at the top. Values inside bars are the daily average concentrations ( $\mu\text{g m}^{-3}$ ) of each species.

Title Page

Abstract

Introduction

Conclusions

References

Tables

Figures

◀

▶

◀

▶

Back

Close

Full Screen / Esc

Printer-friendly Version

Interactive Discussion

SSA and  
heterogeneous  
chemistry in polluted  
coastal areas

E. Athanasopoulou et al.

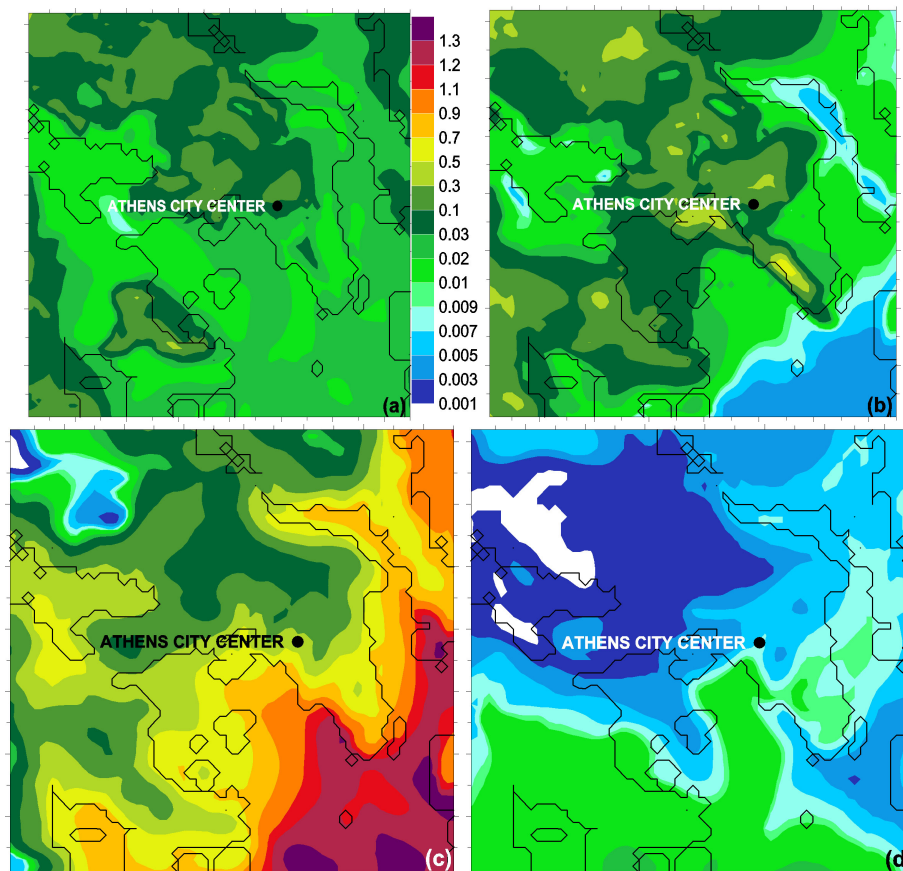


**Fig. 9.** Daily average fine (upper part) and coarse (lower part) nitrate concentration fields ( $\mu\text{g m}^{-3}$ ) in the nested domain. **(a)** and **(c)**: hybrid (base-case) approach, **(b)** and **(d)**: bulk-equilibrium approach.

[Title Page](#)[Abstract](#)[Introduction](#)[Conclusions](#)[References](#)[Tables](#)[Figures](#)[◀](#)[▶](#)[◀](#)[▶](#)[Back](#)[Close](#)[Full Screen / Esc](#)[Printer-friendly Version](#)[Interactive Discussion](#)